Kinetic Analysis of Dynamic ^{13}C NMR Spectra: Metabolic Flux, Regulation, and Compartmentation in Hearts

Xin Yu,* Lawrence T. White,* Chris Doumen,‡ Lisa A. Damico,* Kathryn F. LaNoue,‡ Nathaniel M. Alpert,§ and E. Douglas Lewandowski*

*NMR Center and §PET Center, Department of Radiology, Massachusetts General Hospital and Harvard Medical School, Boston, Massachusetts, and ‡Department of Physiology, Hershey Medical Center, Pennsylvania State University, Hershey, Pennsylvania, USA

ABSTRACT Control of oxidative metabolism was studied using ^{13}C NMR spectroscopy to detect rate-limiting steps in ^{13}C labeling of glutamate. ^{13}C NMR spectra were acquired every 1 or 2 min from isolated rabbit hearts perfused with either 2.5 mM [2-^{13}C]acetate or 2.5 mM [2-^{13}C]butyrate with or without KCl arrest. Tricarboxylic acid cycle flux (V_{TCA}) and the exchange rate between α-ketoglutarate and glutamate (F_1) were determined by least-square fitting of a kinetic model to NMR data. Rates were compared to measured kinetics of the cardiac glutamate-oxaloacetate transaminase (GOT). Despite similar oxygen use, hearts oxidizing butyrate instead of acetate showed delayed incorporation of ^{13}C label into glutamate and lower V_{TCA}, because of the influence of β-oxidation: butyrate = 7.1 ± 0.2 μmol/min/g dry wt; acetate = 10.1 ± 0.2; butyrate + KCl = 1.8 ± 0.1; acetate + KCl = 3.1 ± 0.1 (mean ± SD). F_1 ranged from a low of 4.4 ± 1.0 μmol/min/g (butyrate + KCl) to 9.3 ± 0.6 (acetate), at least 20-fold slower than GOT flux, and proved to be rate limiting for isotope turnover in the glutamate pool. Therefore, dynamic ^{13}C NMR observations were sensitive not only to TCA cycle flux but also to the interconversion between TCA cycle intermediates and glutamate.

INTRODUCTION

^{13}C NMR spectroscopy of tissue metabolism has been applied to numerous living systems and has generated widespread interest for application to laboratory investigations of intact organs and in vivo animal models. An important early contribution was the kinetic modeling of tricarboxylic acid (TCA) cycle flux via ^{13}C labeling within glutamate as detected in in vitro spectra of tissue extracts from different time points (Chance et al., 1983). Such work is based largely on previously described patterns of ^{14}C incorporation in metabolites that were determined via traditional, destructive biochemical methods (Kelleher, 1985; Strisower et al., 1952; Weinman et al., 1957). However, the chemical specificity of NMR spectroscopy allows identification of labeled metabolites to be performed on intact tissues. Thus, an attractive feature of using ^{13}C NMR spectroscopy for physiological applications remains the potential for the kinetic analysis of dynamic changes in ^{13}C spectra obtained over time from functioning, intact hearts and in vivo preparations (Lewandowski, 1992b; Weiss et al., 1992; Robitaille et al., 1993a).

Dynamic changes in ^{13}C spectra from intact hearts have been related to different workloads without changes in high-resolution, multiplet structures in spectra from extracts of the same hearts (Lewandowski, 1992b). Such data are dependent on turnover of label within the TCA cycle, and it is tempting to offer such spectra as a means of evaluating TCA cycle flux. However, simply equating isotope turnover to TCA cycle flux does not take advantage of the power and utility of ^{13}C NMR to provide new information not otherwise available from intact tissues using methodologies such as oxygen consumption rates or radiolabeled CO_2 release. Instead, ^{13}C NMR methods can be used to discern other rate-limiting processes through appropriate applications of kinetic modeling schemes.

Because of the low concentrations of TCA cycle intermediates involved in the recycling of label within the glutamate pool, metabolic events more subtle than the simple labeling of glutamate are seldom detected and remain generally overlooked. Because no less than 90% of the glutamate is located in the cytosol (LaNoue et al., 1970) and the labeling of glutamate occurs through isotope exchange with α-ketoglutarate, glutamate labeling remains an indirect indicator of ^{13}C labeling of TCA cycle intermediates. However, the influence of the isotope exchange rate between glutamate and α-ketoglutarate on isotope turnover within the glutamate pool is not well characterized.

Fundamental to such ^{13}C NMR studies has been the assumption that the TCA cycle intermediate, α-ketoglutarate, is in rapid exchange with glutamate, according to earlier work showing chemical equilibrium across the glutamate-oxaloacetate transaminase (GOT) in the heart (Randle et al., 1970). Until now, this assumption has not been tested in intact tissues, although isolated enzyme measurements of liver GOT, the enzyme that catalyzes this reaction, do show that the enzyme has a large V_{max} value (Fahien and Strmecki, 1969a,b). However, less well established is whether metabolite transport across the mitochondrial membrane is negligible in studies of intact tissues. The intra- and extra-mitochondrial glutamate pools are determined by transport of metabolites that is influenced by

Received for publication 27 February 1995 and in final form 27 July 1995.

Address reprint requests to E. Douglas Lewandowski, Ph.D., NMR Center, Massachusetts General Hospital, Building 149, 13th Street, Charlestown, MA 02129. Tel.: 617-726-5639; Fax: 617-726-7422; E-mail: doug@nmr.mgh.harvard.edu.

0006-3495/95/11/2090/00 $2.00

mitochondrial membrane potential and the redox-dependent malate-aspartate shuttle (Safer, 1975). Thus, the evolution of presteady state ^{13}C NMR spectra is unlikely to be determined solely by TCA cycle activity and may, in fact, be dominated by metabolic communication between subcellular compartments. Therefore, this study was aimed at developing dynamic methods of ^{13}C NMR detection and kinetic data analysis to quantify such rate-limiting events within intact hearts.

Experiments were designed to monitor ^{13}C enrichment rates and isotope turnover within the glutamate pool of isolated rabbit hearts. Isotope kinetics were evaluated under conditions of 1) direct entry and rapid turnover of label in the TCA cycle via ^{13}C-enriched acetate and 2) regulated entry of label in the TCA cycle via β-oxidation of ^{13}C-enriched butyrate (Lewandowski et al., 1991a). Dynamic ^{13}C NMR was used to assess the influences of physiological demand and metabolic flux on the turnover of ^{13}C in intact rabbit hearts. Studies were aimed at testing the relative contributions of TCA cycle flux and interconversion of labeled α-ketoglutarate and glutamate to the pre-steady-state evolution of ^{13}C enrichment within the NMR-detectable glutamate pool. ^{13}C enrichment kinetics was evaluated during manipulation of TCA cycle flux secondary to either activity through β-oxidation (acetate versus butyrate) or altered metabolic demand (mechanical work versus basal metabolic state). Additional measurements of cardiac transaminase rates allowed direct comparison to the kinetic NMR data of isotope exchange rates in intact hearts. The findings indicate that kinetic analysis of ^{13}C NMR data is sensitive to both TCA cycle flux and the interconversion of metabolite pools across the mitochondrial membrane, which can be rate limiting.

MATERIALS AND METHODS

Isolated heart model

Hearts were excised from Dutch belted rabbits (550–700g) that were heparinized (1000 units) and anesthetized with sodium pentobarbital (100 mg/kg intraperitoneal injection). Immediately upon excision, the heart was immersed in a solution containing 20 mM KCl and 120 mM NaCl for cardioplegia at 0°C. The aorta was cannulated for retrograde perfusion at 100 cm hydrostatic pressure with a modified Krebs-Henseleit buffer equilibrated with 95% O_2-5% CO_2 at 37°C. The buffer contained (in mM): NaCl 116, KCl 4, $CaCl_2$ 1.5, $MgSO_4$ 1.2, NaH_2PO_4 1.2, and $NaHCO_3$ 25. During preparation, hearts were perfused with buffer containing 5 mM glucose. A latex balloon was placed in the left ventricle and connected to a pressure transducer line and physiograph (Gould, Inc., Cleveland, OH). The balloon was inflated with water to create a diastolic pressure of 5–10 mmHg. Left ventricular developed pressure (LVDP) and heart rate (HR) were continually measured and recorded with the intraventricular balloon. Rate-pressure product (RPp = HR × LVDP) was used as an index of mechanical work. Myocardial oxygen consumption (MVO_2) was calculated from the difference in O_2 content of perfusion medium in the supply line and coronary effluent collected from the pulmonary artery (Neely et al., 1967). Temperature of the hearts was continuously maintained at 37°C by warm air flow controlled at the NMR system console.

Experimental protocol

Four experimental groups were comprised of hearts perfused with: 1) 2.5 mM acetate (n = 5); 2) 2.5 mM butyrate to introduce β-oxidation (n = 6); 3) acetate + 20 mM KCl to achieve basal metabolic state (n = 5); and 4) 2.5 mM butyrate + 20 mM KCl (n = 5). Additional experiments were done with hearts perfused with [2,4-^{13}C]butyrate at normal workload to eliminate the partial labeling of acetyl-CoA from β-oxidation (n = 2). At the start of each protocol, hearts were perfused with either unlabeled acetate or butyrate for 10 min to reach metabolic equilibrium. At this time, a natural abundance ^{13}C spectrum was acquired. The substrate supply was then switched to the corresponding ^{13}C-labeled substrate: either [2-^{13}C]acetate or [2-^{13}C]butyrate (Isotec, Inc., Miamisburg, OH), with or without KCl. Sequential ^{13}C spectra were then acquired every 1.25 (acetate) or 2.5 (butyrate) min until steady-state enrichment was reached. After each perfusion, hearts were freeze-clamped for biochemical assays and high resolution ^{13}C NMR of tissue extracts.

It is necessary to point out that neither acetate nor butyrate is a physiological substrate for the in vivo heart. However, these two substrates present the simplest scenario for studies that aim at the characterization of rate-limiting steps in isotope kinetics, whereas more physiological substrates, such as long-chain fatty acids, would introduce new rate-limiting steps in the incorporation of label into the glutamate pool, i.e., activation and transport of long-chain fatty acids into the mitochondria. Therefore, the choice of acetate and butyrate as the sole exogenous substrate offers a simple, well-controlled model that serves the purposes of this study well.

Dynamic ^{13}C NMR measurements

Perfused hearts were placed within a sample tube in a 20-mm broad-band NMR probe (Bruker Instruments, Billerica, MA), which was situated in a vertical-bore superconducting NMR magnet operating at a field strength of 9.4 T (Bruker Instruments). NMR data were collected with a Bruker 400 MSL NMR spectrometer. Before each experiment, the magnetic field homogeneity was optimized by shimming on the proton signal of water in the sample to a line width of 20–30 Hz.

^{13}C NMR spectra from intact hearts were acquired at 101 MHz with a 45° pulse angle and 2-s recycle time over 24 to 64 scans (1- to 2.5-min period). Bilevel broad-band decoupling at 0.5 W (1.8 s) and 7.0 W (17 μs) was applied to eliminate carbon-proton coupling and to induce nuclear Overhauser enhancement (NOE) without sample heating. The free induction decay (FID) was acquired with an 8K data set. Changes in relative signal intensities due to nuclear Overhauser enhancement or the relaxation effect were negligible under these pulsing conditions (Lewandowski and Hulbert, 1991; Lewandowski et al., 1991b; Malloy et al., 1988). Natural abundance ^{13}C signal was digitally subtracted, and the raw signal was processed by exponential filtering with a line broadening of 20 Hz to enhance the signal-to-noise ratio before being converted into the frequency domain by Fourier transformation. Peak assignments were referenced to the known resonance of the exogenous, ^{13}C-enriched substrate (2-carbon of acetate at 24.1 ppm, 2-carbon of butyrate at 40.2 ppm) and the well-documented glutamate signals (Bailey et al., 1981; Chance et al., 1983). NMR signal intensities were determined for all spectra by curve-fitting each resonance peak with a Lorentzian curve and integrating the area under the fitted curve with NMR-dedicated software (NMR1, Tripos Associates, Inc., St. Louis, MO).

Kinetic analysis of GOT

The exchange of isotope from the TCA cycle to glutamate occurs through a transamination reaction that also involves oxaloacetate and aspartate. Two isoforms of GOT exist, mitochondrial and cytosolic (Michuda and Martinez-Carrion, 1970). However, the reaction rate of this GOT has not been defined for rabbit heart. The kinetic parameters of both GOTs were measured in this study as described below.

Isolated rabbit hearts were perfused with MSEE buffer (225 mM mannitol, 75 mM sucrose, 5 mM MOPS, 0.1 mM EDTA, and 0.2 mM EGTA

at 0°C and pH 7.0). From homogenized tissue, the cytosolic and mitochondrial fractions were separated by differential centrifugation (Berkich et al., 1991). Measurement of protein content per milliliter in the total homogenate and in the supernatant yielded the percentage of supernatant (cytosolic) present in the total rabbit heart homogenate. Measurements of citrate synthase activity (Idell-Wenger et al., 1978) in the total homogenate and the isolated mitochondrial fraction allowed determination of the percentage of mitochondrial protein in the total homogenate. The fraction of mitochondrial protein was determined to be 31%.

The specific activity of cytosolic GOT for synthesis of glutamate and oxaloacetate was measured in 150 mM KCl, 25 mM MOPS, 10 mM Tris, 5 mM NaCl, 0.15 mM NADH, and 2 U/ml malate dehydrogenase (MDH) at pH 7.2. Enzymatic activity in the forward and reverse directions was determined by the change in absorbance at 340 nm or 280 nm, respectively. Mitochondrial GOT activity was determined at pH 7.7 to mimic the mitochondrial matrix (Chacon et al., 1994). Aliquots of mitochondria were pre-incubated with 0.05% Triton X100 to permeabilize the mitochondria.

V_{max} for GOT was determined in the presence of 10 mM aspartate and α-ketoglutarate. The K_m values for both α-ketoglutarate and aspartate concentration were determined in the presence of an excess of one reactant (10 mM) while varying the concentration of the other. The K_m for glutamate was determined by varying glutamate concentration with 2 mM oxaloacetate in the absence of NADH and MDH (Fahien and Strmecki, 1969a).

Tissue chemistry

Acid extracts were obtained from ventricular muscle of hearts perfused in the magnet as previously described (Lewandowski, 1992a,b). Glutamate, α-ketoglutarate, and aspartate contents in myocardium were determined by spectrophotometric or fluorometric techniques (Bergmeyer, 1974; Williamson and Corkey, 1969). Extracts were then lyophilized and reconstituted in 0.5 ml deuterium oxide (D_2O). High-resolution ^{13}C spectra of reconstituted extract material were obtained.

High-resolution ^{13}C NMR

High-resolution ^{13}C NMR spectra of tissue extracts reconstituted in 0.5 ml D_2O were obtained with a 5-mm ^{13}C probe (Bruker Instruments, Billerica, MA). In vitro ^{13}C spectra were collected over 3000 or 6000 scans (45° pulse, 1.8-s recycle time) with broad-band proton decoupling. Samples were spun (20 Hz) to average out field inhomogeneities. The free induction decay (FID) was acquired with a 32K data set and zero filled to 64K to improve spectral resolution. The signal was processed by 2 Hz exponential filtering followed by Fourier transformation. The multiplet structure of the glutamate carbon signal allowed the fraction of 2-carbon-labeled acetyl-CoA entering the TCA cycle (F_c) and the ratio of anaplerotic flux to citrate synthase (y) to be calculated (Malloy et al., 1987, 1988). The amount of glutamate labeled at the 4-carbon position was determined by comparing the signal intensity from the glutamate 4-carbon resonance peak within each ^{13}C spectrum to a standard 100 mM (1.1 mM ^{13}C natural abundance) solution of glutamate. The total ^{13}C-labeled glutamate at the 4-carbon position was then divided by the total tissue concentration of glutamate from enzymatic assay to obtain the fractional enrichment of glutamate at the 4-carbon position (Lewandowski, 1992a,b).

Kinetic model and analysis

Over the course of perfusion with ^{13}C-enriched substrate, incorporation of label into the glutamate pool was detected by ^{13}C NMR. The appearance of resonance peaks that correspond to ^{13}C enrichment at specific carbon positions within the glutamate pool have been described in detail by others (Chance et al., 1983; Lewandowski and Johnston, 1990; Malloy et al., 1988). Detection of the ^{13}C NMR signal from glutamate is based on the relatively high concentration of intracellular glutamate that is in constant exchange with the TCA cycle via α-ketoglutarate. Initial incorporation of label from the oxidation of either [2-^{13}C]acetate or butyrate into the glutamate pool occurs at the 4-carbon position. The recycling of the label places ^{13}C at either the 2- or 3-carbon of glutamate. Labeling is equally probable at the 2- or 3-carbon of glutamate because of the symmetry of the succinate molecule. Although some investigators have reported asymmetric labeling of malate in various mammalian tissues perfused with ^{13}C-labeled propionate (Sherry et al., 1994), this phenomenon has not been observed in NMR experiments involving functioning tissues oxidizing substrates that enter the TCA cycle via acetyl-CoA (Lewandowski, 1992b; Weiss et al., 1992). Because glutamate is largely located in cytosol, whereas the TCA cycle occurs in mitochondria, ^{13}C-enriched α-ketoglutarate is transported out of mitochondria before chemical exchange occurs between α-ketoglutarate and glutamate (Fig. 1 *A*) (LaNoue et al., 1973).

Analysis of metabolic activity was based on observations of pre-steady-state ^{13}C NMR spectra of glutamate reflecting the dynamic labeling pattern described above. A kinetic model was developed to investigate ^{13}C labeling within key metabolic compartments. The model was derived from the simplified metabolic compartment model that includes key, rate-limiting tricarboxylate pools as well as the major contributing amino acid pools, glutamate and aspartate (Fig. 1 *B*). This simplification was justified by comparing the simulated results with that of a more comprehensive model that also includes a succinate and fumarate pool. Analysis is determined at steady-state flux and with constant intermediate pool sizes. Because of the symmetry in 2- and 3-carbon labeling, the model only considers the labeling of 2-carbon while regarding the labeling of 3-carbon as equal to that of 2-carbon. Citrate, α-ketoglutarate, and glutamate pools are further divided into 2 subcompartments to represent ^{13}C labeling at the 2- and 4-carbon positions of each intermediate. Effects of substrate utilization and anaplerosis are also accounted for by incorporating data measured from high-resolution ^{13}C NMR as parameters in the model. Incorporation of unlabeled intermediate through anaplerosis was considered to enter the TCA cycle at malate while efflux of carbon mass (cataplerosis) occurred through the malic enzyme (Kornberg, 1966; Peuhkurinen, 1984; Russell and Taegtmeyer, 1991). Kinetic equations describing pre-steady-state labeling of each compartment were derived by the principle of mass conservation. This kinetic model, comprising nine differential equations, is presented in further detail in the Appendix.

With a single 9×1 vector q to represent the fractional enrichment of each compartment as a function of time, the model can then be described in matrix form as

$$\frac{d}{dt} q = M_{TCA} \cdot q + U_{Acetyl\text{-}CoA}$$

where M_{TCA} is a 9×9 matrix characteristic of the TCA cycle, its elements are dependent on the TCA cycle flux (V_{TCA}), the interconversion rates between the TCA cycle intermediate and glutamate or aspartate (F_1 and F_2), the level of anaplerosis (y), and the concentrations of each metabolite. The input vector, $U_{Acetyl\text{-}CoA}$, is governed by the fraction of ^{13}C-enriched acetyl-CoA entering the TCA cycle through citrate synthase (F_c). The only nonzero element in $U_{Acetyl\text{-}CoA}$ is the one corresponding to the labeling of the 4-carbon position of citrate because all ^{13}C label from the acetyl-CoA 2-carbon enters the TCA cycle through citrate synthase and results in labeling at the 4-carbon position of citrate.

The detected signals in this model are the 2- and 4-carbon enrichment glutamate in the vector. Acetyl-CoA enrichment (F_c) and anaplerosis to citrate synthase ratio (y) were determined from high-resolution NMR spectra of tissue extracts. Glutamate, aspartate, and α-ketoglutarate concentrations were measured by enzymatic assays. Other metabolite concentrations whose values are relatively stable to the changes in TCA cycle flux were taken from literature on hearts perfused under similar substrate conditions: citrate, 2.94 μmol/g dry wt; malate, 0.60; oxaloacetate, 0.04 (Randle et al., 1970; Taegtmeyer, 1983). The effect of possible variations or errors in these pool sizes was evaluated by sensitivity analysis with a 200% change in pool sizes. The results show that changes in these pool sizes will have minimal impact on the labeling kinetics of glutamate. TCA cycle flux (V_{TCA}) and flux of interconversion between TCA cycle intermediates and amino acid pools (F_1 and F_2) were determined by nonlinear

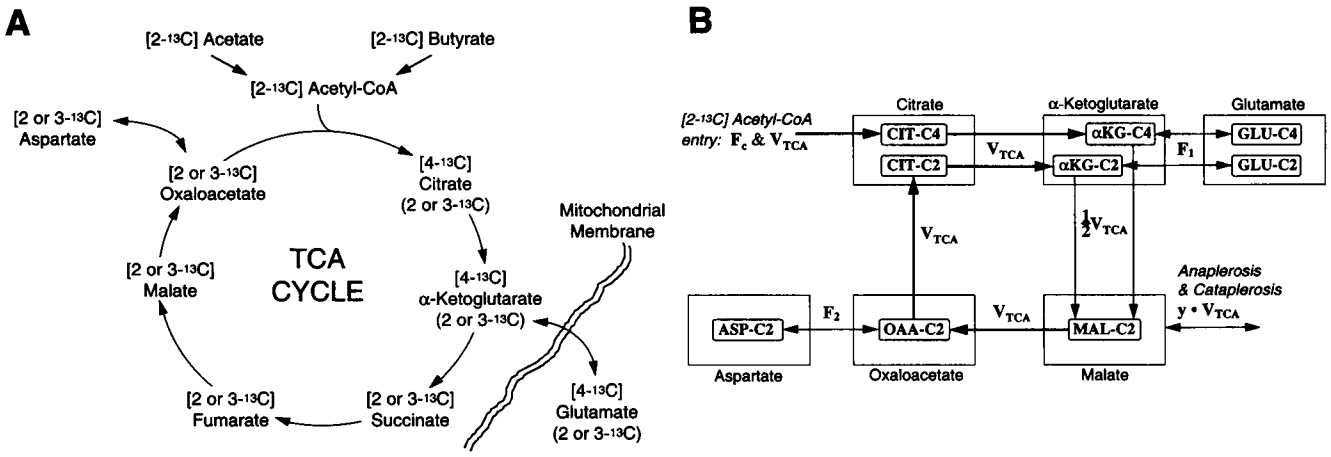

FIGURE 1 Diagram of the TCA cycle. (*A*) Labeling scheme employed in dynamic ^{13}C NMR spectroscopy. Both [2-^{13}C]acetate and [2-^{13}C]butyrate enter the TCA cycle via [2-^{13}C]acetyl-CoA. Initial sites of ^{13}C labeling are at the 4-carbon position of citrate, α-ketoglutarate, and glutamate. Recycling of ^{13}C within TCA cycle results in the labeling of 2- and 3-carbons with equal probability. Note that glutamate, the NMR observable metabolite pool, is located in the cytosol. (*B*) Compartments of metabolic intermediates used in TCA flux analysis. Large boxes represent metabolite pools of or related to TCA cycle. Small boxes represent mathematical compartments of the model. Labeling of 3-carbon is the same as that of 2-carbon and is therefore omitted. Mixing of label occurs after the α-ketoglutarate compartment. Anaplerosis and cataplerosis occur at the malate pool. The kinetic model is composed of nine differential equations describing the labeling kinetics of nine compartments. CIT, citrate; αKG, α-ketoglutarate; GLU, glutamate; MAL, malate; OAA, oxaloacetate; ASP, aspartate. V_{TCA}, TCA cycle flux; F_1, interconversion flux between α-ketoglutarate and glutamate; F_2, interconversion flux between aspartate and oxaloacetate. Note that F_1 and F_2 are not the same as flux through transaminase reactions because transport across mitochondrial membrane is also involved.

least-square fitting of the model to ^{13}C enrichment data from NMR spectra using the Levenberg-Marquardt method. Because alanine and pyruvate concentrations in all four experimental groups were low, alanine aminotransferase activity is minimal. Therefore, the interconversion rates between α-ketoglutarate and glutamate, and between oxaloacetate and aspartate were set equal, i.e., $F_1 = F_2$. The optimization was performed using MATLAB (The MathWorks, Inc., Natick, MA).

Metabolic rates

TCA cycle flux can be calculated from the rate of oxygen consumption (MVO_2) with knowledge of the substrate that is fueling respiration (Kobayashi and Neely, 1979; Randle et al., 1970). For example, for the oxidation of 1 mole of acetate, 3 moles of NADH and 1 mole of $FADH_2$ are generated, which results in the consumption of 2 moles of oxygen. Hence, the turnover of TCA cycle is one-half of the oxygen consumption. In the case of butyrate oxidation, because additional NADH and $FADH_2$ are generated in β-oxidation, the ratio of TCA flux to MVO_2 is 1:2.5 (Fig. 2). Therefore, MVO_2 provided experimental constraints of TCA cycle flux for optimization in kinetic analysis. While the optimal value for TCA cycle flux was obtained from least-square fitting of the model to dynamic ^{13}C NMR observation, a penalty function that reflects the difference between fitted TCA cycle flux and the TCA cycle flux calculated from oxygen consumption was added to the objective function. This allowed the computer to search in a range of estimated TCA cycle flux from oxygen consumption while taking into consideration the measurement error and the oxidation of other fuels.

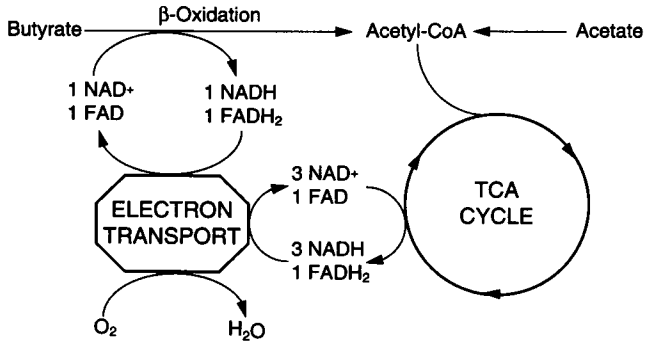

FIGURE 2 Metabolic diagram of acetate and butyrate oxidation. Acetate has direct entry into the TCA cycle via acetyl-CoA. Butyrate, as a four-carbon molecule, undergoes β-oxidation to be cleaved into two acetyl-CoA molecules before entering the TCA cycle. β-Oxidation generates additional reducing equivalents that require oxygen to be reoxidized. Therefore, at the same oxygen consumption rate, TCA cycle flux from butyrate oxidation is slower compared to acetate oxidation, yet the energy yield is the same.

Statistical analysis

All data are presented as mean ± SD. Comparison of intragroup data sets was performed with Student's paired, two-tailed *t*-test. Differences in mean values were considered statistically significant at a probability level of less that 5% ($p < 0.05$).

RESULTS

Contractile function and oxygen consumption

Contractile function, as assessed by rate pressure product (RPP), was similar for hearts at normal workload: 17,100 ± 4,100 beats·mmHg/min for hearts oxidizing acetate, and 19,900 ± 6,400 for hearts oxidizing butyrate. Oxygen consumption (MVO_2) was also similar: 19.4 ± 3.7 μmol/min/g dry wt for the acetate group, and 18.4 ± 3.4 μmol/min/g dry wt for the butyrate group. Hearts arrested with KCl generated no mechanical work. As expected, their oxygen consumption was significantly lower: acetate, 7.5 ± 1.4 μmol/min/g dry wt; butyrate, 6.9 ± 3.0 μmol/min/g dry wt. These results are consistent with both our previous findings

TABLE 1 Steady-state metabolite contents and substrate utilization

	Glutamate	α-Ketoglutarate	Aspartate	F_c (%)	y (%)
Acetate	29.11 ± 2.50	0.50 ± 0.35	1.56 ± 0.80	92.1 ± 6.8	8.9 ± 4.1
Butyrate	26.90 ± 5.59	0.61 ± 0.50	3.27 ± 1.49	47.7 ± 6.2	13.2 ± 4.6
Acetate + KCl	22.64 ± 6.16	0.74 ± 0.09	1.14 ± 0.24	91.9 ± 1.5	11.6 ± 0.9
Butyrate + KCl	22.53 ± 3.58	0.91 ± 0.41	0.95 ± 0.40	47.6 ± 4.9	22.1 ± 11.8

F_c, fraction of ^{13}C-enriched acetyl-CoA entering the TCA cycle. y, ratio of anaplerosis to citrate synthase activity. Values of F_c and y were determined from high-resolution NMR spectra of tissue extracts. Metabolite concentrations are measured by enzymatic assays. All values are given as mean ± SD. Metabolite concentrations are given as μmol/g dry tissue weight.

(Lewandowski, 1992b) and data from canine and rat hearts reported by other investigators (Dean et al., 1990; Bittl and Ingwall, 1985). Thus, the protocol afforded analysis of ^{13}C kinetics at normal and basal metabolic rates in both the absence and presence of significant effects on the TCA cycle flux from additional NADH and $FADH_2$ generation by β-oxidation.

Metabolite content and GOT kinetics

Steady-state metabolite contents are tabulated in Table 1. Values are in agreement with those measured by other investigators for similar experimental conditions (Randle et al., 1970; Taegtmeyer, 1983). There were no statistically significant differences among all four groups. Kinetic parameters of GOT from both cytosol and mitochondria are presented in Table 2.

^{13}C NMR measurements

Proton-decoupled ^{13}C spectra from tissue extracts were similar to those previously presented (Lewandowski et al., 1991a; Lewandowski and Hulbert, 1991; Lewandowski, 1992b). Quantitatively, spectra from KCl-arrested hearts were similar to that of hearts oxidizing the same substrate at normal workload. [2-^{13}C]Butyrate induced a lower level of doublet signal from glutamate 4-carbon resonance because only 50% [2-^{12}C]acetyl-CoA, at most, entered the TCA cycle after butyrate was cleaved into two acetyl-CoA molecules by β-oxidation. The fraction of ^{13}C-enriched acetyl-CoA entering the TCA cycle (F_c) and the ratio of anaplerotic flux to citrate synthase activity (y) calculated from high resolution ^{13}C NMR spectra are presented in Table 1. As expected, F_c values from hearts oxidizing [2-^{13}C]butyrate at both normal workload and during arrest were half that of hearts oxidizing [2-^{13}C]acetate because of the enrichment difference discussed above.

Fig. 3 shows representative, sequential spectra from hearts at normal workloads. Note that incorporation of label into the glutamate pool with [2-^{13}C]butyrate was significantly delayed in reaching steady state as compared to hearts oxidizing [2-^{13}C]acetate. This delay is evident in Fig. 4, which shows the time course of ^{13}C enrichment of glutamate at 2- and 4-carbons from all acquired spectra along with results from least-square fitting.

The delayed approach to steady state of glutamate labeling with hearts oxidizing butyrate was quantitated by the time constants of the labeling curves from a single exponential fit. The time constants for the labeling of glutamate 4- and 2-carbons are as follows: in the acetate group, 7 min for 4-carbon, 17 min for 2-carbon; in the butyrate group, 10 min for 4-carbon, and 32 min for 2-carbon. This delay in glutamate labeling with butyrate oxidation also appears in KCl-arrested hearts as shown in Fig. 4, where the time constants are: with acetate, 14 min for 4-carbon, 46 min for 2-carbon; with butyrate, 21 min for 4-carbon, 97 min for 2-carbon. However, these time constants cannot be used as a direct index of TCA cycle flux because two processes are involved that can affect the labeling kinetics of glutamate—one is TCA cycle activity, the other is exchange of label between α-ketoglutarate and glutamate.

Results from kinetic analysis

Results from least-square fitting of the kinetic model to glutamate labeling are shown in Fig. 4. In all four groups, a precise fit of the model to the experimental data was evi-

TABLE 2 Measured glutamate-oxaloacetate transaminase activity

	Cytosol	Mitochondria
V_{max} (μmol/min/mg total heart protein)	1.62 ± 0.02	1.06 ± 0.05
K_m of α-ketoglutarate (mM)	0.12 ± 0.03	3.22 ± 0.28
K_m of glutamate (mM)	10.69 ± 2.35	32.49 ± 0.98
K_m of aspartate (mM)	2.72 ± 0.08	0.89 ± 0.04

Cytosolic GOT activity was measured at pH = 7.2. Mitochondrial GOT activity was measured at pH = 7.7. All values are given as mean ± SD.

TABLE 3 Flux rates kinetic analysis and GOT measurements

Perfusate supply	V_{TCA}	F_1	F_{GOT}
Acetate	10.1 ± 0.2	9.3 ± 0.6	223
Butyrate	7.1 ± 0.2	6.4 ± 0.5	362
Acetate + KCl	3.1 ± 0.1	5.8 ± 0.6	181
Butyrate + KCl	1.8 ± 0.1	4.4 ± 1.0	158

V_{TCA}, TCA cycle flux. F_1, flux of chemical exchange between glutamate and α-ketoglutarate. F_{GOT}, flux through cytosolic glutamate-oxaloacetate transaminase (GOT). V_{TCA} and F_1 values are determined from kinetic analysis of NMR data and are given as mean ± SD, with the standard deviation calculated from Jacobian matrix of the kinetic model. F_{GOT} values are calculated from measured kinetic parameters of GOT. All flux values are presented as μmol/min/g dry tissue weight.

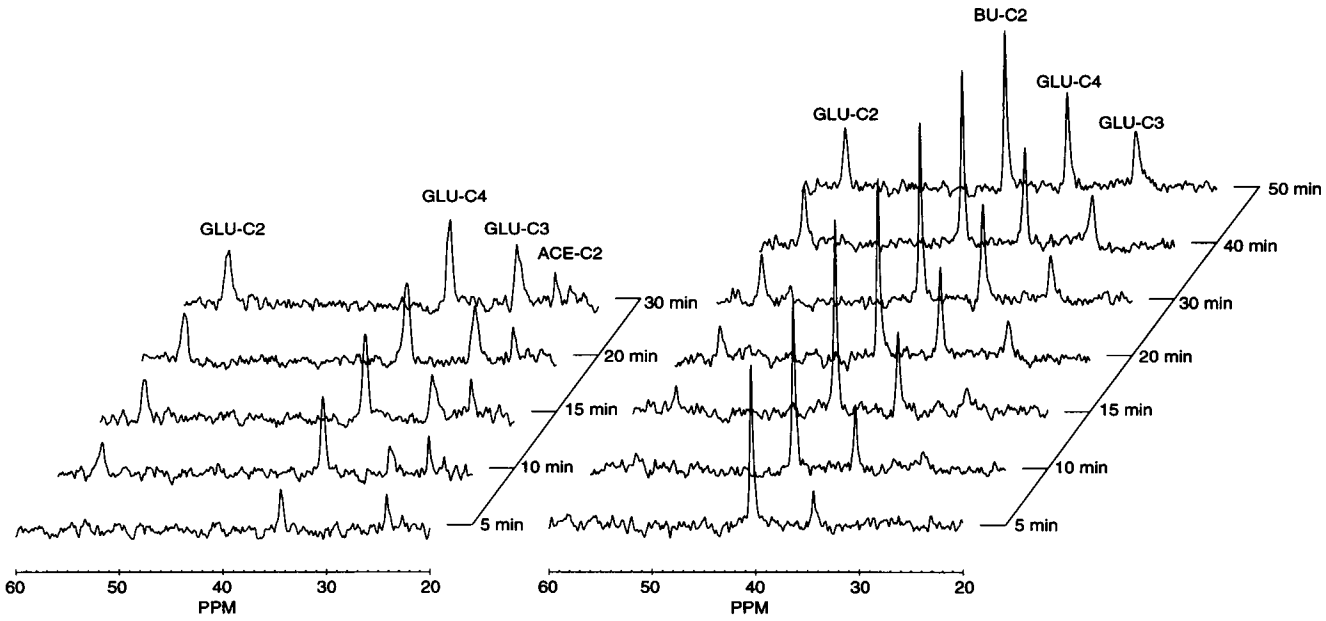

FIGURE 3 Dynamic ^{13}C NMR spectra of isolated rabbit hearts. Spectra are from representative, isolated hearts at normal workload and were acquired during a period of 1 (*left*) or 2.5 (*right*) min. Labeled substrates were 2.5 mM [2-^{13}C]acetate (*left*) and 2.5 mM [2-^{13}C]butyrate (*right*). Heart oxidizing acetate reached steady state in 30 min. Butyrate oxidizing heart reached steady state in 50 min. Identifiable resonance peaks: GLU-C2, 2-carbon of glutamate; GLU-C4, 4-carbon of glutamate; GLU-C3, 3-carbon of glutamate; ACE-C2, 2-carbon of acetate; BU-C2, 2-carbon of butyrate.

dent. TCA cycle flux (V_{TCA}) and F_1 were each determined from nonlinear least-square fitting and are presented in Table 3 with the standard deviation calculated from the Jacobian matrix of the model. KCl-arrested hearts showed significantly reduced TCA cycle flux, only 25–31% of that of hearts at normal workload. On the other hand, hearts oxidizing butyrate also have reduced TCA cycle activity as compared with hearts oxidizing acetate, despite similar oxygen consumption and workload. The result is due to the presence of β-oxidation generating additional reducing equivalents to meet energy demand at a correspondingly lower TCA cycle flux. The exchange rate between α-ketoglutarate and glutamate was also slightly slower in hearts perfused with butyrate. In combination, the reduced TCA cycle flux and the slower interconversion rate accounted for a general delay in the observed ^{13}C enrichment curve from hearts oxidizing butyrate.

To test whether low F_c values can have an impact on the rate of labeling and isotope turnover in glutamate, we also perfused hearts with [2,4-^{13}C]butyrate so that both acetyl-CoA molecules generated from β-oxidation were labeled at the 2-carbon. ^{13}C spectra from tissue extracts showed a heightened doublet signal in the glutamate 4-carbon resonance, resembling that of hearts perfused with [2-^{13}C]acetate. As expected, acetyl-CoA enrichment increased to 92.8%, comparable to that of hearts oxidizing acetate. Yet anaplerosis was similar to hearts perfused with [2-^{13}C]butyrate: y = 13.2%. Despite this high acetyl-CoA enrichment level, the dynamics of glutamate enrichment showed little difference from hearts oxidizing [2-^{13}C]butyrate (Fig. 5). Using the same flux parameters obtained from kinetic analysis of data from the [2-^{13}C]butyrate group, our simulated enrichment curve was in agreement with the experimental data (Fig. 5). Therefore, the observed delay in glutamate labeling from hearts perfused with butyrate was caused by differences in metabolic activity rather than dilution of label, which is consistent with previous findings (Lewandowski and Hulbert, 1991).

Transaminase rates and metabolite compartmentation

Based on measured metabolite contents (Table 1) and kinetic parameters of GOT (Table 2), flux through GOT (F_{GOT}) was calculated according to the double-displacement (ping-pong) reaction kinetics and is presented in Table 3 for comparison to the chemical exchange rate between α-ketoglutarate and glutamate, F_1. Heart protein to tissue weight ratio is 683 mg total heart protein/g dry tissue weight, and the volume to tissue weight ratio is 2 ml/g dry tissue weight (Idell-Wenger et al., 1978), as used for calculation of flux through GOT in Table 3. F_{GOT} was highest in the butyrate group because of the larger mean value for the aspartate pool (Table 1). As shown in Table 3, the F_1 determined from least-square fitting of the model was at least 20 times slower than F_{GOT} in all four groups. F_1 was comparable to TCA cycle flux in hearts at normal workload and was twice the TCA cycle flux in KCl-arrested hearts.

Data fitting was also performed in the absence of the constraint provided by measured oxygen consumption. Removing this constraint allows a 9% deviation in TCA cycle flux and a 14% deviation in F_1 from the values obtained

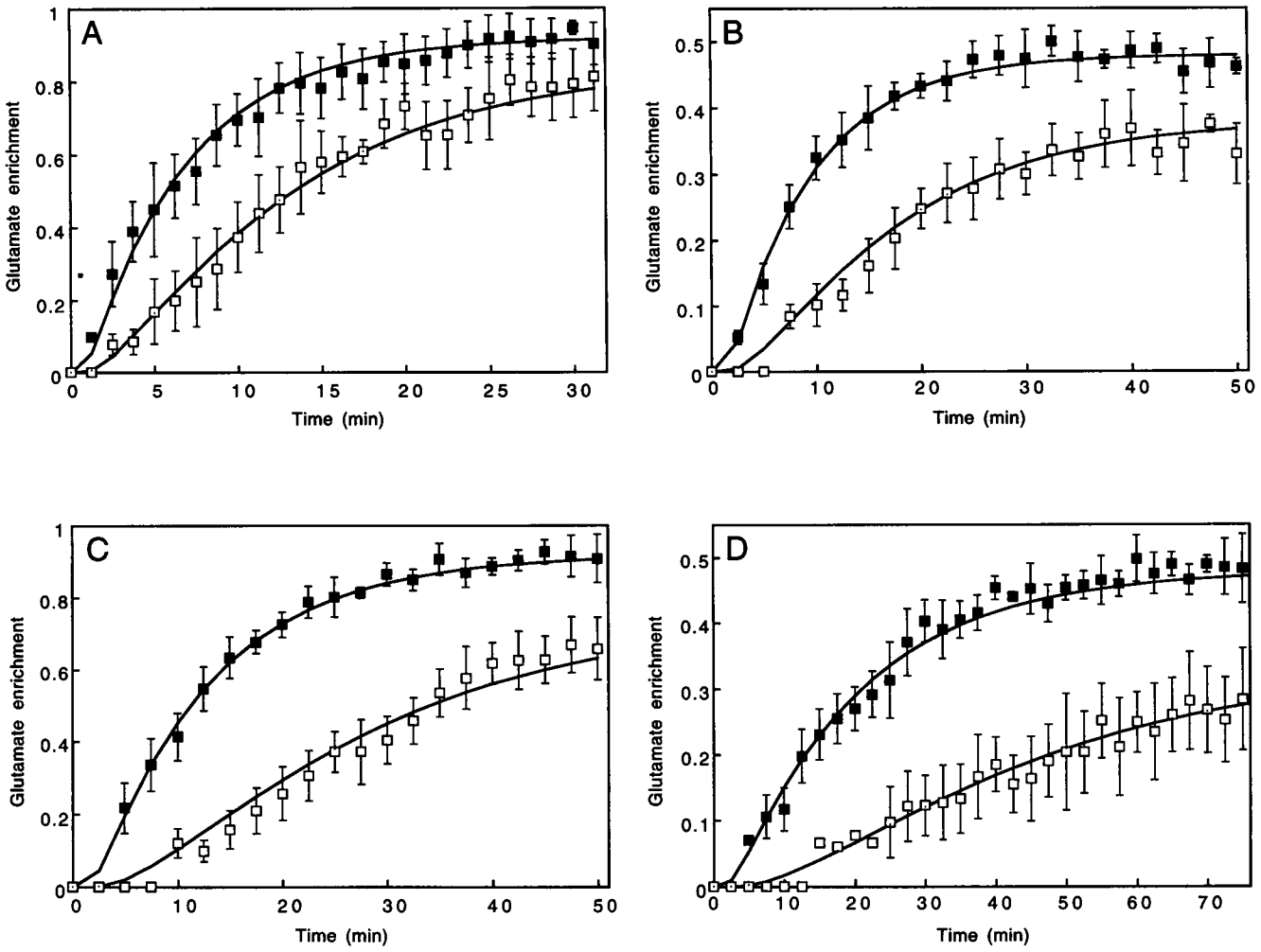

FIGURE 4 Time course of glutamate ^{13}C enrichment from both NMR measurement and kinetic analysis. Signal intensities from dynamic ^{13}C NMR spectra are normalized to steady-state enrichment levels of the 4-carbon of glutamate. NMR data are shown in squares. ■, ^{13}C enrichment level of glutamate at 4-carbon position; □, ^{13}C enrichment level of glutamate at 2-carbon position. Solid lines are modeled enrichment curves from least-square fitting. (*A*) 2.5 mM [2-^{13}C]acetate; (*B*) 2.5 mM [2-^{13}C]butyrate; (*C*) 2.5 mM [2-^{13}C]acetate + 20 mM KCl; (*D*) 2.5 mM [2-^{13}C]butyrate + 20 mM KCl.

from the full model. Even under these unregulated experimental conditions, F_1 remained on the order of TCA cycle flux, significantly lower than the determined GOT flux rate. We also used a fixed TCA cycle flux, calculated from the lower limits of oxygen consumption, so that only F_1 was then fitted to the model, yielding increased F_1 for each group. However, these F_1 values remained an order of magnitude lower than GOT flux. If F_{GOT} alone is used to represent the isotope exchange rate, then simulated enrichment curves showed poor agreement with experimental data. The results of this test are shown in Fig. 6. Therefore, flux through GOT is not the rate-limiting step in the exchange between α-ketoglutarate and glutamate. This slow exchange rate might be a result of metabolite transport due to metabolite compartmentalization, as the TCA cycle enzymes are intramitochondrial and over 90% of glutamate is cytosolic.

Considerations of the model

In our model, ^{13}C label entering the TCA cycle from the acetyl-CoA pool is treated as a step function, i.e., acetyl-CoA is instantly enriched to the level of F_c upon the delivery of ^{13}C enriched substrate. Actually, the time course of acetyl-CoA enrichment occurs as an exponential function of time, where the time constant is the ratio of acetyl-CoA concentration to the flux through the TCA cycle. Because physiological concentrations of acetyl-CoA are approximately 0.2 μmol/g dry wt (Peuhkurinen and Hassinen, 1982), the time constant for the enrichment of acetyl-CoA is very small, from 0.02 to 0.11 min. The enrichment level of acetyl-CoA 10 s after delivery of labeled substrate is already 78% of steady-state values, and by 30 s it is 99%. Thus, the assumption of instant equilibration of acetyl-CoA is a reasonable approximation.

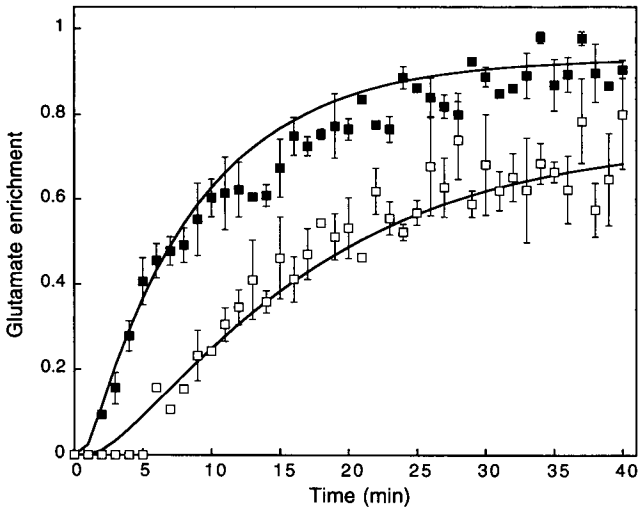

FIGURE 5 Glutamate ^{13}C enrichment from heart oxidizing [2,4-^{13}C]butyrate. Open and closed squares are NMR measured ^{13}C enrichment levels of 2- and 4-carbons of glutamate from hearts perfused with [2,4-^{13}C]butyrate (n = 2). Solid lines are simulated enrichment curves made by using the same flux parameters obtained from kinetic analysis of [2-^{13}C]butyrate data presented in Table 3. The good agreement between simulated curves and experimental data is demonstrated.

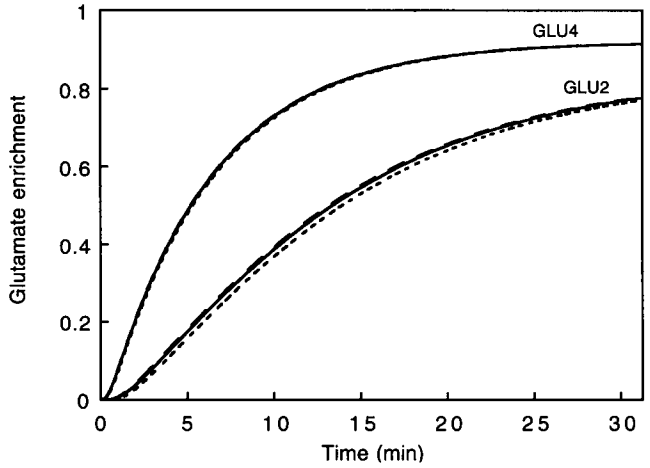

FIGURE 7 Sensitivity analysis. Simulated time course of glutamate enrichment with a simultaneous threefold increase (- - - -) or decrease (– – –) in α-ketoglutarate, malate, and oxaloacetate levels showed little difference from that of measured pool size (——). The minor impact of TCA intermediates on glutamate enrichment demonstrates the robustness of estimated parameters when measurements of TCA cycle intermediates are subject to large statistical fluctuations.

Measurements of the TCA cycle intermediates that are at very low concentrations, α-ketoglutarate, malate, and oxaloacetate, are subject to great statistical fluctuations. To test the robustness of the model to such measurement errors, sensitivity analysis was performed by perturbing the pool size of these compartments by threefold. Fig. 7 shows the simulated time course of glutamate enrichment for measured pool size (solid lines), increased pool size (dotted lines), and decreased pool size (dashed lines). The results, as shown, demonstrate that even the most dramatic changes in pool sizes had little impact on the dynamics of glutamate ^{13}C enrichment. Therefore, pre-steady-state labeling of glutamate is insensitive to changes in α-ketoglutarate, malate, and oxaloacetate at physiological levels.

Our current model is derived from simplified compartmentation of the TCA cycle by eliminating non-rate-limiting pools. To justify this simplification, we have compared simulation results of our reduced model with that of a more comprehensive model that also includes succinate and fumarate pools along with equations to describe both 2- and 3-carbon labeling (8 compartments, 19 differential equations). These two models showed no difference in characterizing the ^{13}C labeling kinetics of glutamate. A closer look at the fractional enrichment of

FIGURE 6 Difference between enzyme rate and interconversion rate. The flux through glutamate-oxaloacetate transaminase (GOT), calculated from measured V_{max} and K_m of GOT as the exchange rate between α-ketoglutarate and glutamate, was used to create the simulated time course of glutamate ^{13}C enrichment (- - - -), which shows very poor agreement with the experimental data (squares, acetate group). ■, measured ^{13}C enrichment level of glutamate at 4-carbon; □, ^{13}C enrichment level of glutamate at 2-carbon. ——, simulated time course of glutamate ^{13}C enrichment using flux parameters determined from kinetic analysis (acetate group).

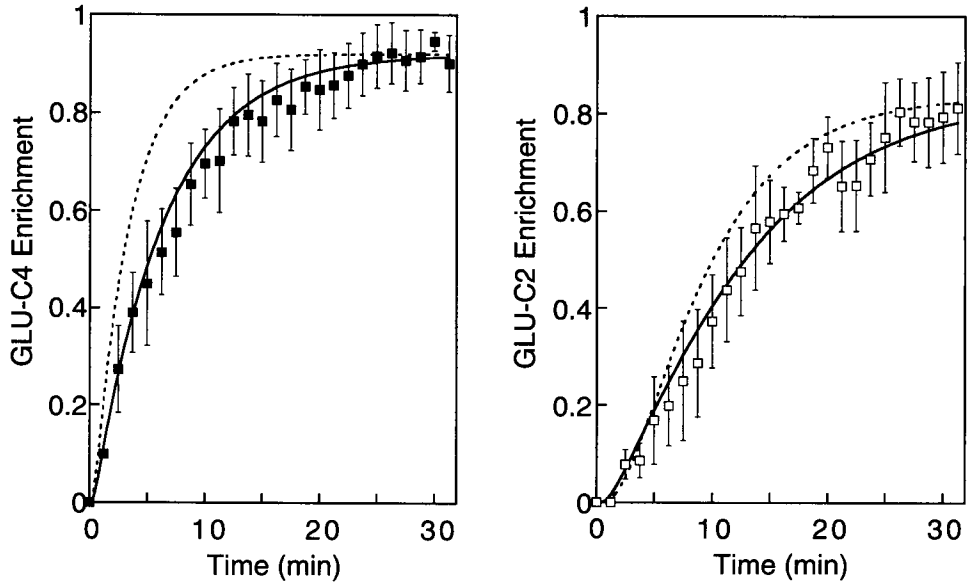

succinate, malate, and fumarate as a function of time shows that the downstream compartment follows the labeling pattern of the previous compartment very closely. This similarity in labeling dynamics of the TCA cycle intermediates is perhaps induced by a relatively large TCA cycle flux as compared to the concentrations of TCA cycle intermediates, which are usually on the order of less than 1 μmol/g dry wt.

DISCUSSION

In this study, changes in oxidative metabolism were studied by ^{13}C NMR spectroscopy at different workload demands and metabolic rates. The influence of the differences in both metabolic rate and control of the turnover of the ^{13}C label within the NMR detectable glutamate pool were systematically examined. Dynamic ^{13}C spectra, reflecting the evolution of enrichment in the glutamate pool, were acquired with 1- or 2-min temporal resolution from intact, functioning hearts. Oxygen consumption and mechanical performance in response to distinctly different physiological demands and metabolic regulation were constantly monitored during the acquisition of NMR spectra. Data acquired in this mode were analyzed with a kinetic model to determine metabolic fluxes and rate-limiting steps. The model for isotope enrichment was tested for sensitivity to metabolite content, respiratory rate, and transaminase activity from four experimental groups. Measured physiological constraints provided the experimental range of data fitting. The model integrates data from enzymatic assays, high-resolution ^{13}C NMR data from tissue extracts, and dynamic changes in ^{13}C NMR spectra from intact hearts to evaluate metabolic regulation in functioning organs. From this study, both TCA cycle flux and the interconversion rate between metabolite pools were determined from the evolution of ^{13}C NMR signals from intact hearts for comparison to experimentally measured enzyme kinetics.

Several previous studies have employed modeling schemes to explore TCA cycle flux and its regulation. These have been based on changes of ^{14}C activity of intermediates (Randle et al., 1970; Nuutinen et al., 1981), tissue clearance of ^{11}C label from PET study (Ng et al., 1994), or ^{13}C enrichment over time of tissue glutamate (Chance et al., 1983; Fitzpatrick et al., 1990; Mason et al., 1992; Weiss et al., 1992; Robitaille et al., 1993b). Our current efforts were not focused toward improving upon existing models of isotope turnover, but rather toward applying a simple model that incorporates a larger number of measured constraints for accurately predicting only the two variables of interest in this study, V_{TCA} and F_1.

Our simplified model is a modification of that developed by Chance et al. (Chance et al., 1983). By considering the total labeling of carbons at 2-, 3-, and 4-carbons instead of individual isotopomer, we were able to take the advantage of the symmetry in isotope labeling at the 2- and 3-carbon positions of the metabolic intermediates to reduce the number of equations necessary to represent the entire model. Consequently, only nine differential equations were needed in representing the kinetics of isotope turnover within the glutamate pool. Sensitivity analysis was also performed to test the robustness of the model to changes in TCA cycle intermediates. By incorporating data from the analysis of high-resolution ^{13}C spectra of heart extracts, anaplerosis and substrate utilization were also accounted for in kinetic analysis, leaving only two parameters to be fitted from the model. Therefore, this model has the advantage of being simple in its formality and yet including as much biological information as possible with a minimal number of adjustable unknowns. This simple model should also be readily applicable to in vivo conditions, provided that constraint parameters are available from appropriate in vivo monitoring and a priori knowledge of metabolite pool sizes.

Oxidative metabolic activity in response to various workloads has been previously investigated by ^{13}C NMR spectroscopy, and delayed incorporation of ^{13}C label into the glutamate pool for hearts at lower workload or basal metabolic state was reported (Lewandowski, 1992b; Weiss et al., 1992). In this study, in addition to changed workload conditions, substrates with different metabolic pathways (β-oxidation versus no β-oxidation) were used to investigate the effect of metabolic control on the kinetics of glutamate enrichment. Hearts oxidizing butyrate showed contractile performance similar to that of hearts oxidizing acetate. The oxygen consumption rate was also similar. When partial labeling of acetyl-CoA from [2-^{13}C]butyrate oxidation was accounted for, the utilization of exogenous substrate for both substrates was also similar. Despite all of these similarities, the time course of ^{13}C enrichment in the glutamate pool for hearts oxidizing butyrate showed a significantly delayed approach to the steady state in both normal and KCl-arrested hearts. When [2,4-^{13}C]butyrate was used as the substrate, the fraction of ^{13}C-enriched acetyl-CoA reached the same level as hearts oxidizing [2-^{13}C]acetate, yet kinetics of glutamate enrichment remained unchanged. Because of the additional reducing equivalents generated in β-oxidation, hearts perfused with butyrate had a slower TCA cycle flux than hearts oxidizing acetate at the same respiratory rate. In addition, the interconversion rate between α-ketoglutarate and glutamate determined from kinetic analysis was also slightly slower with hearts perfused with butyrate. The reduced TCA cycle flux and interconversion rate gave rise to the delayed incorporation of label into the glutamate pool observed in hearts perfused with butyrate.

Substrate utilization and relative flux of anaplerosis were also determined from high-resolution NMR spectra of tissue extracts in this study. Whereas substrate utilization was found to be the same for both short-chain fatty acids regardless of working conditions, the ratio of anaplerosis to citrate synthase activity (y) increased slightly when butyrate was used as the substrate (Table 1). However, care must be taken in interpreting y values, which is an index of relative

contribution of anaplerosis to TCA cycle activity. Although y increased slightly when butyrate was supplied, the calculated anaplerotic flux ($y \times V_{TCA}$) was similar to that of hearts oxidizing acetate at the same working condition: acetate, 0.90 μmol/min/g dry tissue weight; butyrate, 0.94; acetate with KCl, 0.36; butyrate with KCl, 0.40. Therefore, hearts at basal metabolic state may have a relatively lower anaplerotic flux because of a lower energy requirement.

An important consideration is that earlier applications of ^{13}C dynamics have not included potential rate-limiting steps beyond that of TCA cycle flux (Chance et al., 1983; Fitzpatrick et al., 1990; Mason et al., 1992). Although a potential effect of the transaminase rate on glutamate labeling has been experimentally demonstrated by Weiss, et al. with a transaminase inhibitor (Weiss et al., 1995), the physical compartmentation of the glutamate and TCA cycle intermediates must also be considered. This is important because the GOT enzyme is not allosterically regulated and the reaction rate is governed by the specific activity of the enzyme in the myocardium and the concentrations of the reactants in the tissue. Indeed, our characterization of the glutamate-oxaloacetate transaminase kinetics shows the reaction rate of the transaminase to be at least 20 times higher than the TCA cycle turnover (Table 3). However, kinetic analysis of glutamate labeling of intact hearts has suggested a significantly slower exchange rate between α-ketoglutarate and glutamate. It is on the order of TCA cycle flux in all four experimental groups. Because most of the tissue glutamate is located in the cytosol whereas the TCA cycle enzymes are located in mitochondria, there is membrane transport involved in addition to chemical exchange. Therefore, the findings of this study suggest that the slower exchange rate found in intact hearts is due to transport of α-ketoglutarate across the mitochondrial membrane.

If the exchange of label between α-ketoglutarate and glutamate is rate limiting, then the rate of isotope enrichment of glutamate will not precisely reflect rates of isotope incorporation into the TCA cycle intermediates. Fig. 8 *A* shows the simulated time course of ^{13}C enrichment for both glutamate and α-ketoglutarate by using flux parameters determined from the acetate group. It is obvious that presteady-state enrichment of glutamate has a significant delay as compared to the enrichment of α-ketoglutarate. Although only the group of hearts oxidizing acetate at normal workload is shown, the other three groups showed similar delay in glutamate enrichment. Furthermore, because α-ketoglutarate is in constant chemical exchange with glutamate, its labeling kinetics is ultimately determined by both TCA cycle flux and the exchange rate between glutamate and α-ketoglutarate. Therefore, even the enrichment of α-ketoglutarate cannot be simply regarded as an index of the TCA cycle. As can be seen from Fig. 8 *B*, the time course of α-ketoglutarate enrichment is very different from that of citrate, in which enrichment is determined solely by TCA cycle flux.

Evidence that glutamate is largely cytosolic is as follows. Transport of glutamate into heart mitochondria occurs almost exclusively via the glutamate/aspartate exchange transporter (LaNoue and Schoolwerth, 1979; Tischler et al., 1976). Thus, the total of glutamate plus aspartate content in mitochondria is constant at approximately 12 nmol/mg mitochondrial protein (LaNoue et al., 1970), or 3.6 μmol/g dry heart weight. This is the maximum number for mitochondrial glutamate, whereas the total is 22–29 μmol/g dry heart weight. Thus, a very large fraction of the glutamate pool is located in the cytosol, and NMR detection of isotope exchange between glutamate and α-ketoglutarate relies on the efflux of α-ketoglutarate from the mitochondria to the cytosol. The efflux of α-ketoglutarate is accompanied by

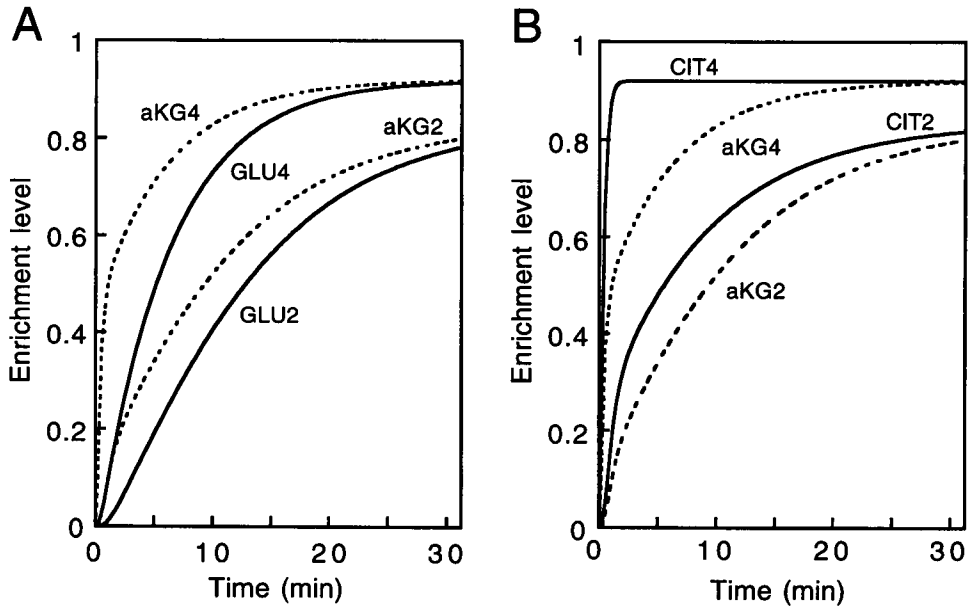

FIGURE 8 Simulated time course of ^{13}C enrichment of citrate, α-ketoglutarate, and glutamate. Flux parameters are determined from least-square fitting of the kinetic model to NMR data in hearts oxidizing [2-^{13}C]acetate at normal workload. Differences in the enrichment kinetics between glutamate (——) and α-ketoglutarate (- - - -) (*A*), and between citrate (——) and α-ketoglutarate (- - - -) (*B*) are demonstrated here.

malate influx through an electroneutral malate-α-ketoglutarate antiport carrier in the malate-aspartate shuttle system (Safer, 1975).

The interaction of the malate-aspartate shuttle with the TCA cycle provides a likely mechanism for the communication and coordination between mitochondrial and cytosolic metabolism (LaNoue and Williamson, 1971). The relatively slow interconversion rate that was observed in the current set of experiments could be due to the influence of the malate-aspartate shuttle, which transports several of the intermediates involved in the exchange of label. The process may be further influenced by shifts in the balance of these intermediates in response to changes in intracellular redox state (Lewandowski et al., 1995). Although the involvement of malate-aspartate shuttle in the exchange of label between glutamate and α-ketoglutarate is appreciated by some investigators (Robitaille et al., 1993b; Chatham et al., 1995), this study represents the first experimental evidence that this process is another rate-limiting step in determining the enrichment rate of glutamate. Thus, dynamic observations of intact tissues with ^{13}C NMR spectroscopy offer the opportunity to explore metabolic regulation at the level of both TCA cycle flux and the communication between intra- and extramitochondrial compartments.

We have used metabolite contents in the whole cell as our pool sizes in the kinetic model, making the tacit assumption that the gradients of these metabolites across the mitochondrial membrane are not large. Distribution of metabolites between the mitochondria and cytosol has been measured in perfused livers (Soboll et al., 1980) by using techniques that are difficult to apply to myocytes. These direct measurements in fact have never been made on heart tissue. However, conclusions can be drawn about the size of these metabolite gradients from studies of isolated mitochondria where the mitochondria have been rapidly separated from media for analysis (LaNoue et al., 1973), or where the NMR signal of metabolites inside the mitochondria can be distinguished from NMR signals of the external metabolites (Masiakos et al., 1991; Hutson et al., 1992). From these studies, the mitochondrial gradient of TCA cycle intermediates and glutamate and aspartate can be considered to be lower in heart than in liver. In the liver, a proton-linked, glutamate transporter permits the formation of a glutamate gradient that is proportional to a pH gradient. The activity of this transportor is very low in heart, to the extent that glutamate influx into the mitochondria is determined by exchange of glutamate for aspartate. In liver, a transporter exchanges dicarboxylic acids for phosphate across a phosphate gradient that is supported by a pH gradient (Masiakos et al., 1991; Hutson et al., 1992). However, the activity of the phosphate/dicarboxylate in heart is very low and TCA cycle intermediates cross the mitochondrial membrane only via exchange with each other. Therefore, our assumption that the total intermediate pools can be used as estimates of cytosolic fractions is validated.

Because glutamate and aspartate can be both mitochondrial and cytosolic, the interconversion rate between glutamate and α-ketoglutarate is really a lumped factor that involves both transaminase flux and transport rate. In the calculation of transaminase flux, because of the small mitochondrial space compared to cytosolic space and consistency of the mitochondrial glutamate plus aspartate pool, the majority of the metabolites are located in the cytosol. Data from isolated mitochondria suggest that mitochondrial content of glutamate and aspartate is approximately 12 nmol/mg mitochondrial protein (LaNoue et al., 1970), aspartate alone is 1 nmol/mg (LaNoue et al., 1974), and α-ketoglutarate is 0.4 nmol/mg (LaNoue et al., 1973). This implies that 88% of the aspartate and 85% of the α-ketoglutarate are located in the cytosol. If correction is made according to these values, the calculated transaminase flux in the acetate group would be 202 μmol/min/g dry tissue. This difference is within 10% in all four experimental groups. However, the correction introduced no change to the simulated enrichment curves in Fig. 6 (dotted lines) and therefore still cannot account for the significantly slower interconversion rate determined from kinetic analysis.

In summary, sequential ^{13}C NMR spectra were obtained from intact hearts at either normal workload or basal metabolic state during perfusion with either ^{13}C-enriched acetate or butyrate. A kinetic model was developed for the analysis of ^{13}C enrichment data to evaluate the regulations in oxidative metabolism and to detect rate-limiting steps in glutamate enrichment. From this analysis, the interconversion between glutamate and α-ketoglutarate was found to be slow relative to the transaminase rate from measured enzyme kinetics. Thus, the exchange of the glutamate pool with TCA cycle intermediates is influenced by rate-limiting processes beyond mere chemical exchange across enzymatic reactions. The implication of these results is that ^{13}C NMR is sensitive not only to TCA cycle activity but also to transport processes for isotope exchange across the mitochondrial membrane. We believe this finding provides a valuable new tool in ^{13}C NMR for monitoring a subcellular process that previously could only be studied in isolated mitochondria.

APPENDIX

The mathematical model used for kinetic analysis is derived from a simplified compartment model of the TCA cycle, including the following key metabolite pools: citrate, α-ketoglutarate, malate, oxaloacetate, glutamate, and aspartate (Fig. 1 *B*). Instead of taking each isotopomer as a single compartment as proposed by Chance et al. (1983), this model is based on a series of compartments including only the total labeling of ^{13}C at either the 2-, 3-, or 4-carbon positions of each metabolite as individual compartments. A further simplification was made by eliminating those equations describing the enrichment of 3-carbon due to the symmetry of 2- and 3-carbon labeling. Therefore, the model has nine compartments in total, as shown in small boxes in Fig. 1 *B*. By the principle of mass conservation, the labeling history of the metabolites can be characterized by a group of nine differential equations incorpo-

rating both TCA cycle flux and interconversion rates between metabolite pools:

$$\frac{d}{dt}\text{CIT4} = \frac{V_{TCA}}{[\text{CIT}]} \cdot (F_c - \text{CIT4})$$

$$\frac{d}{dt}\alpha\text{KG4} = \frac{V_{TCA}}{[\alpha\text{KG}]} \cdot \text{CIT4} - \frac{V_{TCA} + F_1}{[\alpha\text{KG}]} \cdot \alpha\text{KG4} + \frac{F_1}{[\alpha\text{KG}]} \cdot \text{GLU4}$$

$$\frac{d}{dt}\text{GLU4} = \frac{F_1}{[\text{GLU}]} \cdot (\alpha\text{KG4} - \text{GLU4})$$

$$\frac{d}{dt}\text{CIT2} = \frac{V_{TCA}}{[\text{CIT}]} \cdot (\text{OAA2} - \text{CIT2})$$

$$\frac{d}{dt}\alpha\text{KG2} = \frac{V_{TCA}}{[\alpha\text{KG}]} \cdot \text{CIT2} - \frac{V_{TCA} + F_1}{[\alpha\text{KG}]} \cdot \alpha\text{KG2} + \frac{F_1}{[\alpha\text{KG}]} \cdot \text{GLU2}$$

$$\frac{d}{dt}\text{GLU2} = \frac{F_1}{[\text{GLU}]} \cdot (\alpha\text{KG2} - \text{GLU2})$$

$$\frac{d}{dt}\text{MAL2} = \frac{V_{TCA}}{[\text{MAL}]} \cdot \left[\frac{1}{2} \cdot \alpha\text{KG2} + \frac{1}{2} \cdot \alpha\text{KG4} - (1 + y) \cdot \text{MAL2}\right]$$

$$\frac{d}{dt}\text{OAA2} = \frac{V_{TCA}}{[\text{OAA}]} \cdot \text{MAL2} - \frac{V_{TCA} + F_2}{[\text{OAA}]} \cdot \text{OAA2} + \frac{F_2}{[\text{OAA}]} \cdot \text{ASP2}$$

$$\frac{d}{dt}\text{ASP2} = \frac{F_2}{[\text{ASP}]} \cdot (\text{OAA2} - \text{ASP2})$$

Here, CIT, αKG, GLU, MAL, OAA, and ASP denote the metabolites citrate, α-ketoglutarate, glutamate, malate, oxaloacetate, and aspartate, respectively. [CIT], [αKG], [GLU], [MAL], [OAA], and [ASP] are the total pool sizes of the corresponding metabolites. *XXXn* is the dimensionless fractional enrichment level of ^{13}C of certain metabolite at the *n*th carbon position. For example, CIT4 is the fractional enrichment level of ^{13}C at the 4-carbon position of citrate, i.e.,

$$\text{CIT4} = \frac{[\{4 - {}^{13}\text{C}\}\text{CIT}]}{[\text{CIT}]}$$

V_{TCA} is the TCA cycle flux. F_1 and F_2 are the fluxes of interconversion, including both transamination and membrane transport, between α-ketoglutarate and glutamate, and between aspartate and oxaloacetate respectively. Pool sizes are expressed as μmol/g dry wt, and flux values are in μmol/min/g dry wt.

This work was supported by National Heart, Lung, and Blood Institute grant RO1HL49244 (E.D.L.) and was done during the tenure of an Established Investigator Award from the American Heart Association to E.D.L.

REFERENCES

Bailey, I. A., D. G. Gardian, P. M. Matthews, G. K. Radda, and P. J. Seeley. 1981. Studies of metabolism in the isolated, perfused rat heart using ^{13}C NMR. *FEBS Lett.* 123:315–318.

Bergmeyer, H. U. 1974. Methods of Enzymatic Analysis. Academic Press, New York.

Berkich, D. A., G. D. Williams, P. T. Masiakos, M. B. Smith, P. D. Boyer, and K. F. LaNoue. 1991. Rates of various reactions catalyzed by ATP synthase as related to the mechanism of ATP synthesis. *J. Biol. Chem.* 266:123–129.

Bittl, J. A., and J. S. Ingwall. 1985. Reaction rates of creatine kinase and ATP synthesis in the isolated rat heart: a ^{31}P NMR magnetization transfer study. *J. Biol. Chem.* 260:3512–3517.

Chacon, E., J. M. Reece, A.-L. Nieminen, G. Zahrebelski, B. Herman, and J. J. Lemasters. 1994. Distribution of electrical potential, pH, free Ca^{2+}, and volume inside cultured adult rabbit cardiac myocytes during chemical hypoxia: a multiparameter digitized confocal microscopic study. *Biophys. J.* 66:942–952.

Chance, E. M., S. H. Seeholzer, K. Kobayashi, and J. R. Williamson. 1983. Mathematical analysis of isotope labeling in the citric acid cycle with applications to ^{13}C NMR studies in perfused rat hearts. *J. Biol. Chem.* 258:13785–13794.

Chatham, J. C., J. R. Forder, J. D. Glickson, and E. M. Chance. 1995. Calculation of absolute metabolic flux and the elucidation of the pathways of glutamate labeling in perfused rat heart by ^{13}C NMR spectroscopy and nonlinear least squares analysis. *J. Biol. Chem.* 270: 7999–8008.

Dean, E. N., M. Shalafer, and J. M. Nicklas. 1990. The oxygen consumption paradox of "stunned myocardium" in dogs. *Basic Res. Cardiol.* 85:120–131.

Fahien, L. A., and M. Strmecki. 1969a. Studies of gluconeogenic mitochondrial enzymes. II. The conversion of α-ketoglutarate by bovine liver mitochondrial glutamate dehydrogenase and glutamate-oxaloacetate transaminase. *Arch. Biochem. Biophys.* 130:456–467.

Fahien, L. A., and M. Strmecki. 1969b. Studies of gluconeogenic mitochondrial enzymes. III. The conversion of α-ketoglutarate to glutamate by bovine liver mitochondrial glutamate dehydrogenase and glutamate-oxaloacetate transaminase. *Arch. Biochem. Biophys.* 130:468–477.

Fitzpatrick, S. M., H. P. Hetherington, K. L. Behar, and R. G. Shulman. 1990. The flux from glucose to glutamate in the rat brain in vivo as determined by ^{1}H-observed, ^{13}C-edited NMR spectroscopy. *J. Cereb. Blood Flow Metab.* 10:170–179.

Hutson S. M., G. D. Williams, D. A. Berkich, K. F. LaNoue, and R. W. Briggs. 1992. A ^{31}P NMR study of mitochondrial inorganic phosphate visibility effects of Ca^{++}, Mn^{++}, and the pH gradient. *Biochemistry.* 31:1322–1330.

Idell-Wenger, J. A., L. W. Grotyohann, and J. R. Neely. 1978. Coenzyme A and carnitine distribution in normal and ischemic hearts. *J. Biol. Chem.* 253:4310–4318.

Kelleher, J. A. 1985. Analysis of tricarboxylic acid cycle using [^{14}C] citrate specific activity ratios. *Am. J. Physiol.* 248:E252-E260.

Kobayashi, K., and J. R. Neely. 1979. Control of maximum rates of glycolysis in rat cardiac muscle. *Circ. Res.* 44:166–175.

Kornberg, H. L. 1966. Anaplerotic sequences and their role in metabolism. *In* Essays in Biochemistry. P. N. Campbell and G. D. Greville, editors. Academic Press, New York. 1–31

LaNoue K. F., J. Bryla, and D. J. P. Bassett. 1974. Energy-driven aspartate efflux from heart and liver mitochondria. *J. Biol. Chem.* 249: 7514–7521.

LaNoue, K. F., W. J. Nicklas, and J. R. Williamson. 1970. Control of citric acid cycle activity in rat heart mitochondria. *J. Biol. Chem.* 245: 102–111.

LaNoue, K. F., and A. C. Schoolwerth. 1979. Metabolite transport in mitochondria. *Annu. Rev. Biochem.* 48:871–922.

LaNoue, K. F., E. I. Walajtys, and J. R. Williamson. 1973. Regulation of glutamate metabolism and interactions with the citric acid cycle in rat heart mitochondria. *J. Biol. Chem.* 248:7171–7183.

LaNoue, K. F., and J. R. Williamson. 1971. Interrelationships between malate-aspartate shuttle and citric acid cycle in rat heart mitochondria. *Metabolism.* 20:119–140.

Lewandowski, E. D., and D. L. Johnston. 1990. Reduced substrate oxidation in postischemic myocardium: ^{13}C and ^{31}P NMR analyses. *Am. J. Physiol.* 258:H1357–H1365.

Lewandowski, E. D. 1992a. Metabolic heterogeneity of carbon substrate utilization in mammalian heart: NMR determination of mitochondrial versus cytosolic compartmentation. *Biochemistry.* 31:8916–8923.

Lewandowski, E. D. 1992b. Nuclear magnetic resonance evaluation of metabolic and respiratory support of work load in intact rabbit hearts. *Circ. Res.* 70:576–582.

Lewandowski, E. D., M. Chari, R. Roberts, and D. Johnston. 1991a. NMR studies of β-oxidation and short chain fatty acid metabolism in supporting improved contractile recovery of reperfused myocardium. *Am. J. Physiol.* 261:H354-H363.

Lewandowski, E. D., L. A. Damico, L. T. White, and X. Yu. 1995. Cardiac responses to induced lactate oxidation: NMR analysis of metabolic equilibria. *Am. J. Physiol.* In press.

Lewandowski, E. D., and C. Hulbert. 1991. Dynamic changes in ^{13}C NMR spectra of intact hearts under conditions of varied metabolic enrichment. *Magn. Reson. Med.* 19:186–190.

Lewandowski, E. D., D. Johnston, and R. Roberts. 1991b. Effects of inosine on glycolysis and contracture during myocardial ischemia. *Circ. Res.* 68:578–587.

Malloy, C. R., A. D. Sherry, and F. M. Jeffrey. 1987. Carbon flux through citric acid cycle pathways in perfused heart by ^{13}C NMR spectroscopy. *FEBS Lett.* 212:58–62.

Malloy, C. R., A. D. Sherry, and F. M. H. Jeffrey. 1988. Evaluation of carbon flux and substrate selection through alternate pathways involving the citric acid cycle of the heart by ^{13}C NMR spectroscopy. *J. Biol. Chem.* 263:6964–6971.

Masiakos, P. T., G. D. Williams, D. A. Berkich, M. B. Smith, and K. F. LaNoue. 1991. ^{31}P NMR saturation transfer study of the in situ kinetics of the mitochondrial adenine nucleotide translocase. *Biochemistry.* 30: 8351–8357.

Mason, G. F., D. L. Rothman, K. L. Behar, and R. G. Shulman. 1992. NMR determination of the TCA cycle rate and α-ketoglutarate/glutamate exchange rate in rat brain. *J. Cereb. Blood Flow Metab.* 12:434–447.

Michuda, C. M., and M. Martinez-Carrion. 1970. The isozymes of glutamate-aspartate transaminase: mechanism of inhibition by dicarboxylic acids. *J. Biol. Chem.* 245:262–269.

Neely, J., H. Liebermeister, E. Battersby, and H. Morgan. 1967. Effect of pressure development on oxygen consumption by isolated rat heart. *Am. J. Physiol.* 212:804–814.

Ng, C. K., S.-C. Huang, H. R. Schelbert, and D. B. Buxton. 1994. Validation of a model for [1-^{11}C] acetate as a tracer of cardiac oxidation metabolism. *Am. J. Physiol.* 266:H1304–H1315.

Nuutinen, E. M., K. J. Peuhkurinen, E. P. Pietilainen, J. K. Hiltunen, and I. E. Hassinen. 1981. Elimination and replenishment of tricarboxylic acid-cycle intermediates in myocardium. *Biochem. J.* 194:867–875.

Peuhkurinen, K. J. 1984. Regulation of the tricarboxylic acid cycle pool size in heart muscle. *J. Mol. Cell Cardiol.* 16:487–495.

Peuhkurinen, K. J., and I. E. Hassinen. 1982. Pyruvate carboxylation as an anaplerotic mechanism in the isolated perfused rat heart. *Biochem. J.* 202:67–76.

Randle, P. J., P. J. England, and R. M. Denton. 1970. Control of the tricarboxylate cycle and its interactions with glycolysis during acetate utilization in rat heart. *Biochem. J.* 117:677–695.

Robitaille, P.-M. L., D. P. Rath, A. M. Abduljalil, J. M. O'Donnell, Z. Jiang, H. Zhang, and R. L. Hamlin. 1993a. Dynamic ^{13}C NMR analysis of oxidative metabolism in the in vivo canine myocardium. *J. Biol. Chem.* 268:26296–26301.

Robitaille, P.-M. L., D. P. Rath, T. E. Skinner, and A. M. Abduljalil. 1993b. Transaminase reaction rates, transport activities and TCA cycle analysis by post-steady state ^{13}C NMR. *Magn. Reson. Med.* 30:262–266.

Russell, R. R., and H. Taegtmeyer. 1991. Changes in citric acid cycle flux and anaplerosis antedate the functional decline in isolated rat hearts utilizing acetoacetate. *J. Clin. Invest.* 87:384–390.

Safer, B. 1975. The metabolic significance of the malate-aspartate cycle in heart. *Circ. Res.* 37:527–533.

Sherry, A. D., B. Sumegi, B. Miller, G. L. Cottam, S. Gavva, J. G. Jones, and C. R. Malloy. 1994. Orientation-conserved transfer of symmetric Krebs cycle intermediates in mammalian tissue. *Biochemistry.* 33: 6268–6275.

Soboll S., R. Elbers, R. Scholz, and H. W. Heldt. 1980. Subcellular distribution of di- and tricarboxylates and pH gradients in perfused rat liver. *Hoppe-Seylers Z. Physiol. Chemie.* 361:69–76.

Strisower, E. H., G. D. Kohler, and I. L. Chaikoff. 1952. Incorporation of acetate carbon into glucose by liver slices from normal and alloxan-diabetic rats. *J. Biol. Chem.* 198:115–126.

Taegtmeyer, H. 1983. On the inability of ketone bodies to serve as the only energy providing substrate for rat heart at physiological work load. *Basic Res. Cardiol.* 78:435–450.

Tischler, M., J., Pachence, J. R. Williamson, and K. F. LaNoue. 1976. Mechanism of glutamate-aspartate translocation across the mitochondrial membrane. *Arch. Biochem. Biophys.* 173:448–461.

Weinman, E. O., E. H. Strisower, and I. L. Chaikoff. 1957. Conversion of fatty acids to carbohydrate: application of isotopes to this problem and role of the Krebs cycle as a synthetic pathway. *Physiol. Rev.* 37: 252–272.

Weiss, R. G., S. T. Gloth, R. Kalil-Filho, V. P. Chacko, M. D. Stern, and G. Gerstenblith. 1992. Indexing tricarboxylic acid cycle flux in intact hearts by carbon-13 nuclear magnetic resonance. *Circ. Res.* 70:392–408.

Weiss, R. G., M. D. Stern, C. P. de Albuquerque, K. Vandegaer, V. P. Chacko, and G. Gerstenblith. 1995. Consequences of altered aspartate aminotransferase activity on ^{13}C-glutamate labelling by the tricarboxylic acid cycle in intact rat hearts. *Biochim. Biophys. Acta.* 1243:543–548.

Williamson, J. R., and B. E. Corkey. 1969. Assays of intermediates of the citric acid cycle and related compounds by fluorometric enzyme methods. *In* Methods in Enzymology. J. M. Colowick, editor. Academic Press, New York. 434–514.